Mechanical Technology and Engineering Insights

www.mtei.reapress.com

Mech. Technol. Eng. Insights. Vol. 1, No. 4 (2024) 187–197.

Paper Type: Original Article

Experimental and Numerical Investigation of Grain Refinement in Low Carbon Steel Sheets During Constrained Groove Pressing

Faeze Nejati[1,*], Soheila Sojoodi[2]

[1] Department of Civil Engineering, Ayandegan Institute of Higher Education, Tonekabon, Iran; civilnj1998@gmail.
[2] Department of Mechanical Engineering, University of Guilan, Rasht, Iran; soheila_sojodi@yahoo.com.

Citation:

Received: 17 January 2024 *Revised: 13 May 2024* *Accepted: 26 August 2024*	Nejati, F., & Sojoodi, S. (2024). Experimental and numerical investigation of grain refinement in low Carbon steel sheets during constrained groove pressing. *Mechanical Technology and Engineering Insights, 1*(4), 187-197.

Abstract

In the current research work, an Ultrafine-Grained (UFG) microstructure was fabricated in low-carbon steel sheets using the Constrained Groove Pressing (CGP) technique, a state-of-the-art method for producing small grain sizes via Severe Plastic Deformation (SPD). The dies for the CGP were designed and fabricated taking into account the principles of CGP (groove angle of 45° and groove width and depth equal to the sheet thickness, 2 mm). A finite element analysis was performed in 2D plane-strain mode using ABAQUS to examine the distribution of effective plastic strain. Sheets of low-carbon steel measuring 102×50×2 mm³ underwent up to four CGP passes. Properties such as hardness and tensile strength were assessed using the Vickers hardness test and the tensile test (as per the guidelines of ASTM E8M). Optical microscopy was performed to analyze the microstructural evolution in accordance with ASTM standards E03-1, E407-99, and E112. The simulation results showed that, on average, an effective strain of approximately 1.15 per pass can be achieved. Grain diameter was found to decrease from 22.5 µm (ASTM grain size number 8) in the as-received state to 4.5 µm (ASTM number 13.5) after four passes, with an 80% reduction. The increase in hardness was observed to range from 52 HV to 252 HV, representing a 385% improvement. It was proved that the Hall-Petch relation holds with the linear fit ($R^2 > 0.98$). This shows that grain refinement is the major strengthening parameter. From both experimental and FEA results, it can be concluded that the CGP process is highly efficient for obtaining ultra-fine-grained sheets with improved mechanical properties.

Keywords: Constrained groove pressing, Low-carbon steel, Ultrafine-grained microstructure, Finite element simulation, Grain refinement, Mechanical properties.

1 | Introduction

UFG materials would definitely play an important role in the future of industrialization on Earth due to their unique mechanical and physical properties. There are several techniques and methods through which these

Corresponding Author: civilnj1998@gmail
https://doi.org/10.48313/mtei.v1i4.64

kinds of materials were produced [1]. The SPD process, widely regarded as an effective technique for producing Nanostructured/UFG materials, has enabled their production. In the SPD process, the grain size of materials is reduced to the nanoscale, thereby improving mechanical properties. According to the Hall-Petch relation, a reduction in grain size normally increases material strength.

The fabricated materials produced through the bottom-up approach are rarely used in industry due to their porous nature. Conversely, in the case of a top-down process, nanostructured materials are fabricated using plastic deformation processes. The fabricated materials produced by such severe plastic deformations play an important role owing to their non-porous nature, high strength and toughness, and suitable dimensions for performing mechanical/physical tests. To date, several techniques have been introduced for fabricating ultrafine-grained materials. The most suitable technique depends on the type of materials used for the fabrication process. However, some of these techniques, such as equal channel angular pressing [2], [3] and high-pressure torsion [4], [5] can be used only for bulk metals. In contrast, other techniques, including repetitive corrugation and straightening [6], [7], accumulative roll bonding [8], [9] constrained Groove rolling [10], and Constrained Groove Pressing (CGP), are suitable for producing nanocrystalline sheets. Among all these techniques, the CGP method was first introduced by Shin et al. [11] and is exclusively designed for sheet metals, with several advantages compared to other SPD techniques.

In the CGP process, the sheets undergo considerable shear deformation using grooves and flat dies alternately [12]. The imposition of this amount of shear plastic deformation on the sheet results in enhanced mechanical properties of the sheet material, including strength, mean hardness, and grain refinement, as reported in recent studies [13–15].

According to recent experimental studies, there have been notable grain refinement and enhanced mechanical properties of the material [12], [13], [15]. In recent times, the CGP process has been studied using different materials, including aluminum [14], copper sheets [16], and brass [17]. It is necessary to note that finite element analyses and experimental studies have been conducted to investigate the performance of various new processes, such as the semi-CGP process [18] and the rubber pad CGP process [19]. Moreover, comparative studies have been conducted to assess the performance of the RCS and CGP processes, and the results clearly indicate that the CGP process is superior to the repetitive corrugation and straightening process [20].

Several experiments have demonstrated that CGP is a reliable technique for optimizing the microstructure and improving the mechanical properties of low-carbon steel sheets. According to Alihosseini and Dehghani [21], CGP could efficiently refine the coarse-grained structure to ultra-fine grain (260–270 nm), yield strength up to 563 MPa after three passes, and enhance bake hardenability by 170 percent compared with their coarse-grained counterparts. Moreover, the study by Khodabakhshi and Kazeminezhad [22] showed that the CGP process considerably increases dislocation density and electrical resistivity by up to 100%. In the same vein, the work by Khodabakhshi et al. [23] demonstrated that CGP-processed UFG low-carbon steel exhibits a reduced work-hardening rate but enhanced strain-rate sensitivity.

Regarding new process modification techniques, Kumar [24] proposed cross-route-Constrained Groove Pressing (cross-CGP). Cross-CGP is a process optimization approach to enhance strain homogeneity and improve the mechanical properties of low-carbon steel sheets. The results showed that the tensile strength and hardness of low-carbon steel sheets processed using the cross-CGP technique are greater than those of conventional CGP, particularly at higher pass numbers.

Kumar [25], in an extensive review of developments in CGP, discussed recent advancements in CGP modification techniques, including improved die designs, annealing techniques, cross-CGP, ring CGP, hybrid SPD, covered-sheet case CGP, and rubber pad CGP, among others.

Regarding the numerical simulations, Khodabakhshi et al. [26] carried out three-dimensional finite element modeling of the CGP-cross route procedure. They demonstrated that the values and uniformity of strain and hardness distributions obtained by FEM simulations agreed with experimental findings for low-carbon steel sheets. Using DEFORM-3D software, Singh et al. [27] conducted numerical simulations of the CGP of 316

austenitic stainless steel (and hence extended to low-carbon steel) and confirmed that the yield strength values calculated using analytical models agreed well with experimental findings.

More recently, Abdian and Kazeminezhad [28] reported the influence of inter-pass and first inter-pass annealing on the properties of low carbon steels after the CGP procedure, revealing that performing inter-pass annealing in the temperature range of 300–500 °C keeps hardness (160–170 Vickers) constant with the increment of CGP passes, and the elongation loss rate gets reduced. Moreover, Poojitha et al. [29] revealed that a combination of CGP followed by cold rolling reduced grain size to ~0.3 μm and increased yield strength to ~483 MPa for annealed ARMCO Fe low-carbon steel, starting from 90 MPa.

Satjabut et al. [30] conducted a study on the use of CGP prior to intercritical annealing in dual-phase steels. They observed that martensitic and tempered martensitic starting structures yield DP steels with an appropriate strength-elongation relationship.

Hence, even after several studies, there is still a need for experiments, along with finite element analysis, specifically conducted on low-carbon steel sheets after repeated applications of CGP, with attention to strain distribution, microstructural development, and mechanical behavior. The current work is dedicated to fulfilling this requirement by designing suitable CGP dies, performing two-dimensional finite element analysis using ABAQUS, and conducting tensile and hardness tests.

2|CGP DIE Design Consideration

In the CGP method, two sets of dies are used: grooved dies to impose severe plastic deformation, and flattening dies to straighten the sheet. As illustrated in *Fig. 1*, according to the principles of the CGP process, the width and height of the die grooves must equal the sheet thickness, and the groove angle must be 45° to achieve pure shear deformation. These design dimensions result in a pure shear strain of $\gamma=1.15$ (equivalent von Mises strain of $\varepsilon=0.58$) in the deformed regions.

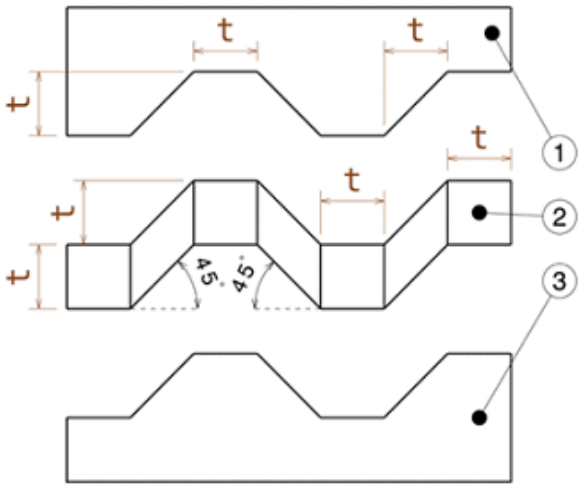

Fig. 1. Equal dimensions of sheet thickness and the groove height and width, and the distances between grooves (part 1: Upper die-- part 2: Sheet-- part 3: Lower die).

Referring to *Eqs. (1)-(5)*, it is proved that the applied Von Mises effective strain in the deformed areas in each step of the pressing process is equal to 0.58. It must be noted that the process is considered to be performed under plane-strain conditions.

Referring to *Eqs. (1)-(5)*, it can be shown that the von Mises effective strain induced in the deformed areas during each pressing step is equal to 0.58. It should be noted that the process is assumed to occur under plane strain conditions. The shear strain γ is related to the groove angle θ.

$$\gamma_{xy} = \frac{x}{t} = \frac{t}{t} = 1. \quad (1)$$

$$\varepsilon_{xy} = \frac{\gamma_{xy}}{2} = \frac{1}{2}. \quad (2)$$

$$\varepsilon_x = \varepsilon_y = \varepsilon_z = \varepsilon_{yz} = \varepsilon_{zx} = 0. \quad (3)$$

$$\varepsilon_{eff} = \sqrt{\frac{2}{9}\left[(\varepsilon_x - \varepsilon_y)^2 + (\varepsilon_y - \varepsilon_z)^2 + (\varepsilon_z - \varepsilon_x)^2\right] + \frac{4}{3}\left[{\varepsilon_{xy}}^2 + {\varepsilon_{zy}}^2 + {\varepsilon_{zx}}^2\right]}. \quad (4)$$

$$\varepsilon_{eff} = \sqrt{\frac{4{\varepsilon_{xy}}^2}{3}} = \sqrt{\frac{4(\gamma_{xy}/2)^2}{3}} = \frac{1}{\sqrt{3}} = 0.58. \quad (5)$$

Since any change in the specimen's dimensions can hinder the imposition of plastic strain and the attainment of high cumulative strain, most SPD methods are designed to keep the specimen's overall dimensions unchanged. As shown in *Fig. 2*, one complete pass of the CGP process consists of four pressing stages, each inducing a strain of 0.58 in the deformed regions. Upon completion of these four stages, a relatively uniform strain is introduced throughout the entire sheet, thereby finishing one CGP pass.

As proven above, pressing a plate-shaped workpiece using the grooved die imposes an effective strain of 0.58 in the deformed regions. In the second stage (the flattening step), the workpiece is flattened using a set of flattening dies; consequently, the inclined regions are subjected to a reverse effective strain of 0.58 again. At the end of this step, the sheet contains two distinct types of regions: 1) regions with an effective strain of 1.16, and 2) unstrained regions (zero strain). These regions alternate with a spacing equal to the sheet thickness. In *Fig. 2*, the white regions represent zero-strain areas, while the black regions indicate areas with an induced strain of 1.16.

The specimen is then rotated 180° about the axis perpendicular to the sheet plane and subjected to *Eqs. (1)-(5)* again. Finally, during the fourth stage (flattening of the corrugated sheet), a uniform strain of 1.16 is induced throughout the entire sheet.

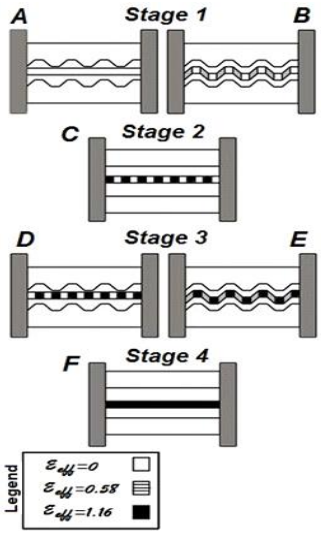

Fig. 2. The schematic illustration of the sequence of the CGP technique.

3|Experimental and Finite Element Procedures

To study the impact of the CGP process on sheet deformation and to calculate plastic strains, FE analysis was performed under plane-strain conditions using ABAQUS. To reduce the time required for simulation and calculation and to obtain accurate results, all dies were modeled as analytical rigid bodies. Meshing of the sheet was done using CPE4R elements, i.e., 4-node bilinear plane-strain quadrilateral elements with reduced integration. The total number of two-dimensional elements used to discretize the sheet is 984, and the total number of nodes is 1017. A friction coefficient of 0.1 was considered, which falls within the acceptable range of 0.05-0.1.

All dies used in the CGP processing of low-carbon steel sheets have been designed and manufactured in accordance with the guidelines for CGP processing. The dimensions of the cavity in which the specimens are inserted are identical to those of sheet specimens. Sheets of low-carbon steel, measuring 102 mm x 50 mm x 2 mm, have been selected as the raw material.

To examine the influence of CGP processing on low-carbon steel sheets subjected to different pass-number processes, tensile and hardness tests were performed under identical conditions. Tensile test specimens in accordance with ASTM E8M were prepared from sheets subjected to varying numbers of passes. Hardness testing was conducted in the thickness direction of both deformed and as-received sheets.

Grain size in the specimens was determined before and after the CGP technique across various numbers of passes. For this reason, the specimens were prepared and polished in accordance with the standards ASTM E03 1 and ASTM E407 99, respectively. Grain size measurements were performed in accordance with ASTM E112 using images taken with an optical microscope at a magnification of 400×. The validation of the FEA model was reported in a previously published paper [18].

4|Results and Discussion

The results are divided into three subsections: Effective strain distribution from finite element simulation, microstructural evolution and grain size, and hardness measurements.

4.1|Effective Strain Distribution

Finite element analysis of the CGP process using ABAQUS was performed in order to analyze the distribution of equivalent plastic strain PEEQ. According to *Eqs. (1)-(5)*, the strain value imposed by every pressing stage is estimated to be 0.58 for the deformed regions; hence, the total accumulated strain in two stages (corrugation followed by flattening) is 1.16, while the accumulated strain in four stages is 2.32.

Fig. 3 depicts the contour plot of the distribution of PEEQ on the sheet surface after the fourth pressing stage. The results from the ABAQUS simulation, in terms of PIEQ values ranging from 1.0 to 36.9 (supplementary legends), indicate a broad range of strains. It is important to note that values exceeding 10 are due to element distortions or incorrect integration-point calculations, which often occur during large-strain SPD simulations. The effective strains in the deformed region range from 1.0 to 2.5. On average, the strain after one pass equals 1.15, whereas the expected value according to theoretical assumptions is 1.16.

Strain non-uniformity can be easily seen; higher strains (PEEQ ≈ 1.5 – 2.5) are found in the regions of the corners of the grooves and close to the sheet surfaces, whereas lower strains (≈1.0 – 1.2) can be noticed in the regions in the center of the sheets and the regions around the tips of the grooves. Such non-uniformity tends to decrease after the second and third passes due to the rotation and repressing operations, as noted by other authors [26], [27].

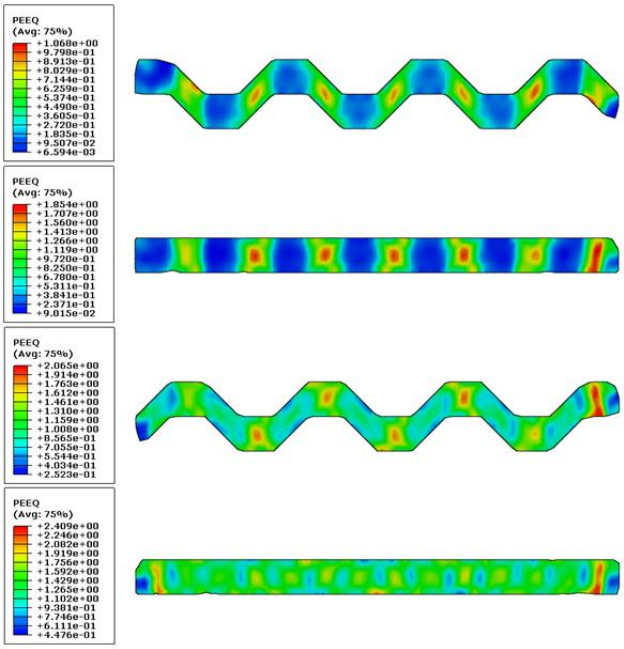

Fig. 3. The schematic illustration of the sequence of the CGP technique.

4.2 | Microstructure and Grain Size Evolution

The optical microstructure of the as-received low-carbon steel sheet is shown in *Fig. 4*. The microstructure is composed of equiaxed grains of ferrite with a uniform distribution pattern. Based on the ASTM E112 standard, the mean grain size number was approximately 8.0. This result means that the mean grain size diameter is roughly 22.5 microns.

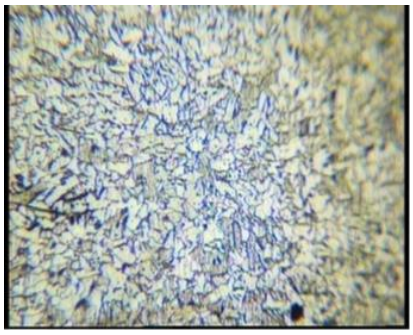

Fig. 4. Microstructure of the as-received low-carbon steel specimen.

The microstructural structures after 1, 2, 3, and 4 CGP passes are shown in *Fig. 5*. As observed from *Fig. 5a*, after the first CGP pass, the microstructure consists of elongated and fragmented equiaxed grains along the shear directions, in addition to the presence of deformation bands and dislocations. At the same time, a few areas contain large grains. The microstructure of the sample after the second CGP pass is fairly homogeneous, as most grains have been refined to the sub-micrometer scale; however, a few elongated coarse grains remain. After the third CGP pass (*Fig. 5c*), a nearly completely UFG microstructure is obtained with average grain sizes less than 10 μm.

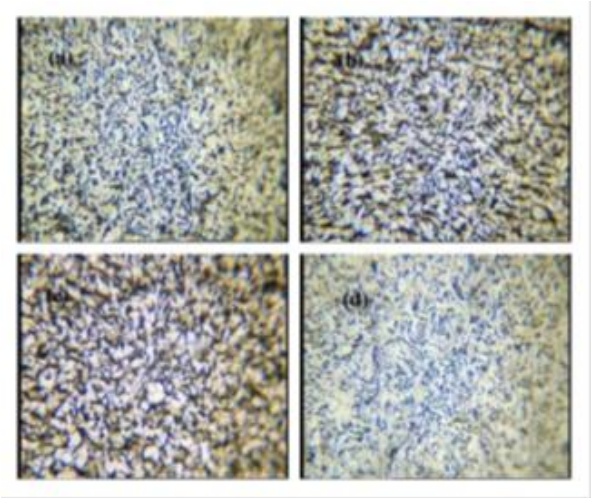

Fig. 5. Microstructures after CGP processing; a. 1 pass, b. 2 passes, c. 3 passes, d 4 passes.

Fig. 6 presents the average ASTM grain size number as a function of the number of pressing passes. Measurements were taken at four different testing points on each specimen to assess homogeneity. The following values are extracted from *Table 1*:

Table 1. Average grain size parameters as a function of the number of CGP passes (based on ASTM E112).

Number of Passes	Grain Size Number (ASTM)	Approx. Average Grain Diameter (μm)
As-received	8.0	22.5
1st pass	10.0	11.2
2nd pass	11.5	6.7
3rd pass	12.5	5.3
4th pass	13.5	4.5

From the graph presented, it is evident that the grain size number increases with each pass, which is equivalent to a decrease in grain size. The largest reduction in grain size occurs between the as-received stage and the first pass (~22.5 μm to ~11.2 μm). Further passes give rise to even more reductions in grain size, although the amount of reduction gets smaller with each consecutive pass. With four passes, the grain size will be reduced by approximately 80%.

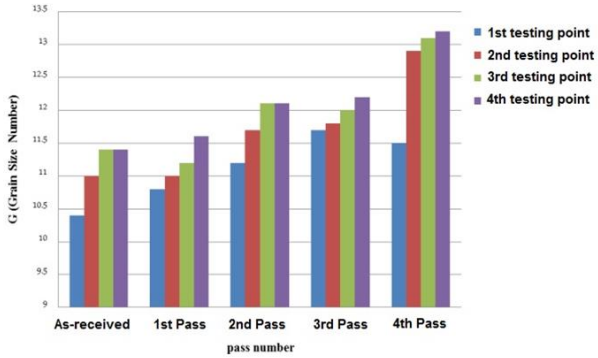

Fig. 6. Average ASTM grain size number versus number of pressing passes for four different testing points.

4.3 | Hardness

Hardness tests were conducted throughout the thickness of the specimens. *Fig. 7* presents the average hardness readings HV as a function of the number of CGP cycles. *Table 2* presents the following readings for the test specimens:

Table 2. Vickers hardness readings for different CGP cycle numbers.

Number of Passes	Mean Hardness (HV)	Increase Relative to As-Received
As-received	~52	–
1st pass	~148	185%
2nd pass	~195	275%
3rd pass	~228	338%
4th pass	~252	385%

The hardness increases rapidly after the first pass due to extensive work hardening and initial grain fragmentation. The second pass raises hardness by an additional 47 HV, the third by 33 HV, and the fourth by 24 HV. The increment diminishes as the pass number increases, indicating a saturation effect. This behavior is consistent with the Hall–Petch relationship: as grain size decreases, hardness increases, but the strengthening effect per unit strain reduces at very fine grain sizes due to the dominance of dislocation-based mechanisms and possible dynamic recovery.

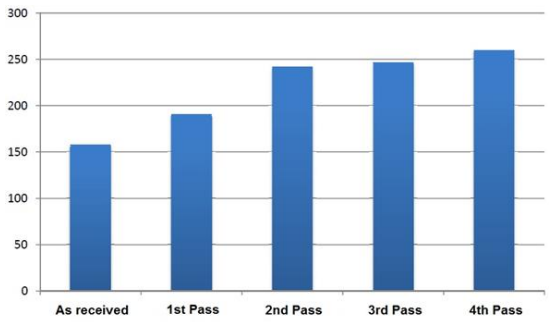

Fig. 7. Mean Vickers hardness value across sheet thickness versus number of CGP passes.

Hardness increases sharply after the first pass due to work hardening and initial grain fragmentation. Hardness increases further by 47 HV during the second pass, by 33 HV during the third pass, and by 24 HV during the fourth pass. The increase diminishes as the number of passes increases, reflecting a saturation effect. This trend is explained by the Hall-Petch equation, which states that the harder a material is, the smaller its grains are. However, beyond certain small grain sizes, the increase in hardness per unit strain becomes less significant due to dislocation mechanisms.

5 | Conclusion

CGP was successfully used on low-carbon steel sheets; finite element simulations and experiments were conducted to examine strain, microstructure, grain refinement, and hardening. The following findings can be made:

I. Design of dies and strain examination: CGP dies with an inclination angle of 45° and groove depths equal to the sheet thickness (2 mm) have been fabricated. The FEA results in ABAQUS showed that the effective strain imposed by each press is roughly 0.58. After four presses (one cycle), the average cumulative effective strain is roughly 1.15, which is close to the theoretical value (1.16). Some strain inhomogeneity (1.0-2.5) was noted at groove corners, and it decreases significantly with increasing number of presses.

II. Microstructural refinement: By the use of an optical microscope, it was found that initial coarse equiaxial ferrite grains (average diameter 22.5 μm, ASTM Grain Size No. 8) become finer progressively through each

cycle, and four passes give rise to an ultrafine-grained structure with an average grain diameter of 4.5 μm (ASTM Grain Size No. 13.5), which indicates a grain size reduction of 80%. Most pronounced refinement takes place in the first pass.

III. Improvement in hardness: Hardness was measured using the Vickers hardness test on the material, and the results indicated a significant increase in hardness from 52 HV in the as-received condition to 148 HV, 195 HV, 228 HV, and 252 HV after the 1st, 2nd, 3rd, and 4th passes, respectively. This result implies an overall increase of 385% in hardness after four passes. The increase in hardness decreased after additional passes due to saturation.

IV. Hall-Petch relationship: There exists a direct linear relationship between Vickers hardness values and the inverse square root of the average grain size ($R^2 > 0.98$). It was therefore concluded that grain refinement is the major hardening process for low-carbon steel samples subjected to the CGP treatment. The Hall-Petch constants were obtained as $HV_0 \approx 20$ HV and $k \approx 18$ HV·$\mu m^{1/2}$.

V. Efficiency of the method: Simulation coupled with experimental results demonstrates that cyclic groove processing is an efficient technique for manufacturing ultrafine-grained steel sheets. Finite element analysis has demonstrated that this severe plastic deformation technique effectively improves both mechanical properties and microstructure while maintaining the sample sheet's dimensions.

Conflict of Interest

The authors report no conflicts of interest related to this work.

Data Availability

All relevant data are presented in this manuscript.

Funding

No financial support was received for the conduct of this study.

References

[1] Valiev, R. Z., Estrin, Y., Horita, Z., Langdon, T. G., Zechetbauer, M. J., & Zhu, Y. T. (2006). Producing bulk ultrafine-grained materials by severe plastic deformation. *JOM*, *58*(4), 33–39. https://doi.org/10.1007/s11837-006-0213-7

[2] Oh, S. J., & Kang, S. B. (2003). Analysis of the billet deformation during equal channel angular pressing. *Materials science and engineering:A*, *343*(1), 107–115. https://doi.org/10.1016/S0921-5093(02)00324-6

[3] Valiev, R. Z., & Langdon, T. G. (2006). Principles of equal-channel angular pressing as a processing tool for grain refinement. *Progress in materials science*, *51*(7), 881–981. https://doi.org/10.1016/j.pmatsci.2006.02.003

[4] Horita, Z., & Langdon, T. G. (2008). Achieving exceptional superplasticity in a bulk aluminum alloy processed by high-pressure torsion. *Scripta materialia*, *58*(11), 1029–1032. https://doi.org/10.1016/j.scriptamat.2008.01.043

[5] Valiev, R. Z., Islamgaliev, R. K., & Alexandrov, I. V. (2000). Bulk nanostructured materials from severe plastic deformation. *Progress in materials science*, *45*(2), 103–189. https://doi.org/10.1016/S0079-6425(99)00007-9

[6] Huang, J. Y., Zhu, Y. T., Jiang, H., & Lowe, T. C. (2001). Microstructures and dislocation configurations in nanostructured Cu processed by repetitive corrugation and straightening. *Acta materialia*, *49*(9), 1497–1505. https://doi.org/10.1016/S1359-6454(01)00069-6

[7] Huang, J., Zhu, Y. T., Alexander, D. J., Liao, X., Lowe, T. C., & Asaro, R. J. (2004). Development of repetitive corrugation and straightening. *Materials science and engineering: a*, *371*(1), 35–39. https://doi.org/10.1016/S0921-5093(03)00114-X

[8] Lee, S. H., Saito, Y., Tsuji, N., Utsunomiya, H., & Sakai, T. (2002). Role of shear strain in ultragrain refinement by accumulative roll-bonding (ARB) process. *Scripta materialia*, *46*(4), 281–285. https://doi.org/10.1016/S1359-6462(01)01239-8

[9] Saito, Y., Utsunomiya, H., Tsuji, N., & Sakai, T. (1999). Novel ultra-high straining process for bulk materials—development of the accumulative roll-bonding (ARB) process. *Acta materialia*, *47*(2), 579–583. https://doi.org/10.1016/S1359-6454(98)00365-6

[10] Lee, J. W., & Park, J. J. (2002). Numerical and experimental investigations of constrained groove pressing and rolling for grain refinement. *Journal of materials processing technology*, *130–131*, 208–213. https://doi.org/10.1016/S0924-0136(02)00722-7

[11] Shin, D. H., Park, J. J., Kim, Y. S., & Park, K. T. (2002). Constrained groove pressing and its application to grain refinement of Aluminum. *Materials science and engineering: A*, *328*(1), 98–103. https://doi.org/10.1016/S0921-5093(01)01665-3

[12] Hosseini, E., Kazeminezhad, M., Mani, A., & Rafizadeh, E. (2009). On the evolution of flow stress during constrained groove pressing of pure copper sheet. *Computational materials science*, *45*(4), 855–859. https://doi.org/10.1016/j.commatsci.2008.12.004

[13] Krishnaiah, A., Chakkingal, U., & Venugopal, P. (2005). Production of ultrafine grain sizes in aluminium sheets by severe plastic deformation using the technique of groove pressing. *Scripta materialia*, *52*(12), 1229–1233. https://doi.org/10.1016/j.scriptamat.2005.03.001

[14] Zrnik, J., Kovarik, T., Novy, Z., & Cieslar, M. (2009). Ultrafine-grained structure development and deformation behavior of aluminium processed by constrained groove pressing. *Materials science and engineering: a*, *503*(1), 126–129. https://doi.org/10.1016/j.msea.2008.03.050

[15] Yoon, S. C., Krishnaiah, A., Chakkingal, U., & Kim, H. S. (2008). Severe plastic deformation and strain localization in groove pressing. *Computational materials science*, *43*(4), 641–645. https://doi.org/10.1016/j.commatsci.2008.01.007

[16] Hosseini, E., & Kazeminezhad, M. (2010). Integration of physically based models into FE analysis: Homogeneity of copper sheets under large plastic deformations. *Computational materials science*, *48*(1), 166–173. https://doi.org/10.1016/j.commatsci.2009.12.023

[17] Mou, X., Peng, K., Zeng, J., Shaw, L. L., & Qian, K. W. (2011). The influence of the equivalent strain on the microstructure and hardness of H62 brass subjected to multi-cycle constrained groove pressing. *Journal of materials processing technology*, *211*(4), 590–596. https://doi.org/10.1016/j.jmatprotec.2010.11.013

[18] Shirdel, A., Khajeh, A., & Moshksar, M. M. (2010). Experimental and finite element investigation of semi-constrained groove pressing process. *Materials & design*, *31*(2), 946–950. https://doi.org/10.1016/j.matdes.2009.07.035

[19] Borhani, M., & Djavanroodi, F. (2012). Rubber pad-constrained groove pressing process: Experimental and finite element investigation. *Materials science and engineering: A*, *546*, 1–7. https://doi.org/10.1016/j.msea.2012.02.089

[20] Solhjoei, N., Varposhty, A. R., Mokhtarian, H., & Manian, A. P. (2014). A comparative study to evaluate the efficiency of rcs and cgp processes. *Indian journal of scientific research (IJSR)*, *1*(2), 563–572. https://api.semanticscholar.org/CorpusID:54881156

[21] Alihosseini, H., & Dehghani, K. (2012). Bake hardening of ultra-fine grained low carbon steel produced by constrained groove pressing. *Materials science and engineering: A*, *549*, 157–162. https://doi.org/10.1016/j.msea.2012.04.024

[22] Khodabakhshi, F., & Kazeminezhad, M. (2011). The effect of constrained groove pressing on grain size, dislocation density and electrical resistivity of low carbon steel. *Materials & design*, *32*(6), 3280–3286. https://doi.org/10.1016/j.matdes.2011.02.032

[23] Khodabakhshi, F., Kazeminezhad, M., & Kokabi, A. H. (2010). Constrained groove pressing of low carbon steel: Nano-structure and mechanical properties. *Materials science and engineering: A*, *527*(16), 4043–4049. https://doi.org/10.1016/j.msea.2010.03.005

[24] Kumar, S. (2023). Strength enhancement and uniform strain distribution through cross route-constrained groove pressing. *IOP conference series: Materials science and engineering*, *1284*(1), 12035. https://doi.org/10.1088/1757-899X/1284/1/012035

[25] Kumar, S. (2023). Developing methods of constrained groove pressing technique: A review. *Proceedings of the institution of mechanical engineers, part l: journal of materials: Design and applications*, *237*(6), 1319–1346. https://doi.org/10.1177/14644207221143358

[26] Khodabakhshi, F., Abbaszadeh, M., Mohebpour, S. R., & Eskandari, H. (2014). 3D finite element analysis and experimental validation of constrained groove pressing–cross route as an SPD process for sheet form metals. *The international journal of advanced manufacturing technology*, *73*(9), 1291–1305. https://doi.org/10.1007/s00170-014-5919-z

[27] Singh, R., Agrahari, S., Yadav, S. D., & Kumar, A. (2021). Microstructural evolution and mechanical properties of 316 austenitic stainless steel by CGP. *Materials science and engineering: A*, *812*, 141105. https://doi.org/10.1016/j.msea.2021.141105

[28] Abdian, M., & Kazeminezhad, M. (2025). The effect of first and repetitive inter-pass annealing during severe plastic deformation on microstructure and mechanical properties of low carbon steel. *Results in materials*, *26*, 100721. https://doi.org/10.1016/j.rinma.2025.100721

[29] Poojitha, V., Raghu, T., & Pandurangadu, V. (2021). Microstructure and mechanical behavior of armco fe severely plastically deformed by combination of constrained groove pressing and cold rolling. *Journal of materials engineering and performance*, *30*(11), 8196–8209. https://doi.org/10.1007/s11665-021-06053-z

[30] Satjabut, P., Kalhor, A., Uthaisangsuk, V., & Mirzadeh, H. (2022). Microstructure and mechanical properties of dual-phase steels by combining adjusted initial microstructures and severe plastic deformation. *Steel research international*, *93*(5), 2100596. https://doi.org/10.1002/srin.202100596